Sports Eng
DOI 10.1007/s12283-013-0116-0

ORIGINAL ARTICLE

Luge track safety

Mont Hubbard

Abstract Simple geometric models of ice surface shapes and equations of motion of objects on these surfaces can be used to explain ejection of sliders from ice tracks. Simulations employing these explain why certain design features can be viewed as proximate causes of ejection from the track and hence design flaws. This paper studies the interaction of a particle model for the luge sled (or its right runner) with the ice fillet commonly connecting inside vertical walls in turns to the flat track bottom. A numerical example analyzes the 2010 luge accident at the Vancouver Olympics. It shows that this runner-fillet interaction, and specifically the fillet's positive curvature up the inside wall, can cause a vertical velocity more than sufficient to clear the outside exit wall. In addition the negative curvature of the fillet along the track and the large vertical velocity, explain loss of fillet or wall contact and slider ejection. This exposes the fillet along inside walls as a track design flaw. A more transparent track design and review process could provide more complete and thorough design and verification scrutiny by competent scientists and engineers without financial involvement or conflicts of interest and potentially lead to safer future designs.

Keywords Luge · Ice track · Safety · Design · Ejection · Accident

1 Introduction

One day before the opening of the 2010 Winter Olympic Games in Vancouver, a tragic crash in the 6th and last training run claimed the life of Georgian luge slider Nodar Kumaritashvili. The accident cast a pall over the impending Olympics and called into question whether one of the centerpieces of the Games, the ice sliding track, was safe enough to proceed.

A series of investigations and reviews followed. Television recordings of the accident were immediately analyzed by the International Luge Federation (FIL). Less than ten hours after the accident the FIL stated that "there was no indication that the accident was caused by deficiencies in the track." FIL representatives instead declared that the athlete was responsible and that the accident was caused by a steering error rather than a track design flaw. Yet several changes were immediately made to the track including: (1) increasing the height of the outside wall by 2.26 m for a distance of 18 m along the track after the exit from curve 16, and by a height of 1 m for an additional 10 m; (2) increasing the height of the inside wall by 0.4 m for 46 m; and (3) "Squaring off the curve of the ice between the base of the track and the side walls of the outrun" [1]. All the Olympic luge events were eventually contested from the lower women's start to limit top speeds.

Since the accident several analyses of it have been published. Within two months an Official Report by FIL [1] appeared. Most of this dealt with athlete qualification procedures, track construction and homologation (certification), and previous crash histories. Although the report at least recognized that this "tragic result ... should not have occurred as a result of an initial driving error" [1], the few sentences dealing with the accident itself offered only a pseudo-scientific explanation: the sled "appears to have hit the wall at an exceptional angle that caused the sled to compress ... result[ing] in the sled serving as a catapult when it decompressed launching ... the sled into the air" [1]. Furthermore it classified the dynamics of the crash as "unknown and unpredictable" [1].

M. Hubbard (✉)
Department of Mechanical and Aerospace Engineering,
University of California, Davis, CA 95616, USA
e-mail: mhubbard@ucdavis.edu

Published online: 27 April 2013

A Coroner's report [2] followed after seven months. It found that there was "no evidence that any serious injury resulted from the initial impact with the inside wall of the track", and it at least correctly recognized that "the collision with the inner wall caused the sled's right runner to ride up onto the wall, causing … the sled to be launched into the air." [2]. It also concluded, qualitatively, that "The bottom inside corner ... had a rounded profile that influenced the rate and angle at which the sled runner climbed the wall, ultimately affecting the trajectory of [the] ejection". The Coroner's report recommended an independent and comprehensive safety audit of the track. This audit was planned and solicited in [3] and has, since the initial review of this paper, finally been released [4].

The accident occurred at the bottom of the track near the exit from the last turn (Turn 16 in Fig. 1) at a near maximum speed of 143.3 kph (39.8 m/s). A particularly clear re-enactment of the preceding sequence of events occurs in [5]. The accident was captured in real time with video footage which can still be viewed [6]. Several consecutive video frames looking up-track at the oncoming sled are shown in Fig. 2. Later analysis [1] concluded that, reacting to perturbations in the previous Turn 15 and to contact of the slider's right glove with the ice during Turn 16, the sled descended the banked portion at the exit of Turn 16 too early, and crossed the flat bottom portion of the track (Fig. 2a). Its right runner then contacted the rounded lower portion of the inner wall (Fig. 2b), and rode up the inner cylindrical wall (Fig. 2c, d) while the left runner continued touching the floor.

The vertical velocity that resulted in slider ejection from the track was acquired entirely during this launch process that occupied at most three frames (less than 0.1 s). Yet nearly three years after the incident, no investigation (including the 18 month long audit [4]) has clearly described how the sled acquired the vertical velocity required for the rider to be ejected, i.e. to clear the outside wall at the exit of the turn. The purpose of this paper is to provide the first actual explanation, based on physical principles, of how the sled and slider were ejected from the track and to explain the track design features responsible. It focuses on the rounded shape of the bottom inside corner. In the remainder of the paper this is called the "fillet". Finally, the paper briefly examines the design and review process as it exists today and makes suggestions to increase track design safety.

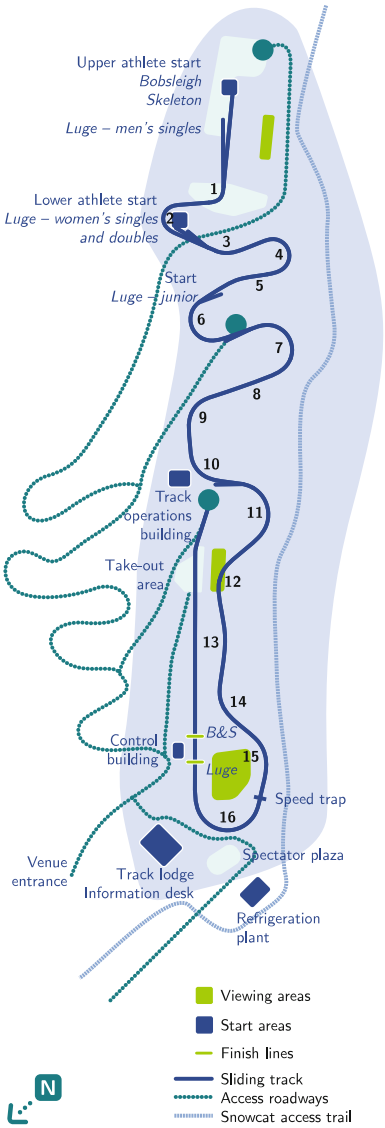

Fig. 1 Plan view of Whistler ice track. The accident occurred at the very bottom of the track on exit from Turn 16 at a speed of 39.81 m/s

2 Methods

2.1 Luge sled description

Before proceeding it should be asked, "What do luge sleds look like?" with a view to whether a particle approximation for its (or its right blade's) motion is a reasonable one. The two steel runners, although not sharpened like ice skate blades, are thin enough that they strongly indent the ice surface. The sled goes where the runners are pointed, and there is usually little if any lateral slip of the runners on the ice. Although the lateral cross section of the runner surface contacting the ice is not exactly circular or even uniform, it suffices to think of it as a surface with major (longitudinal) radius $R_s \simeq 13$ m and minor (lateral) radius $r_s \simeq 0.003$ m. The runner-ice contact patch length has been estimated to be of the order of 12 cm. Luge rules specify that the runner ice contact points may not be separated laterally by more than 0.45 m and that the maximum width of the sled, including shell and handles, must not exceed 0.55 m [7] (Fig. 3). Thus the

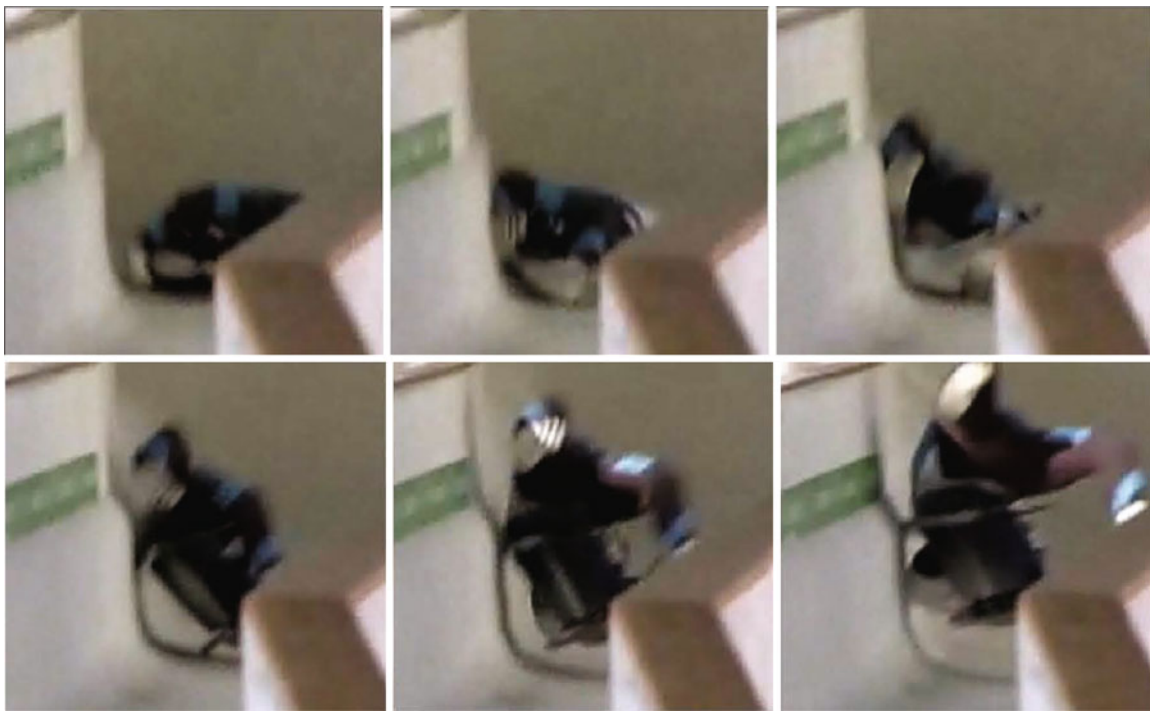

Fig. 2 Sequential frames of accident video of approaching sled (referred to as **a**–**c** on *top* and **d**–**f** on *bottom*) looking up-track into Turn 16 spaced at 0.033 s. The camera axis points roughly from the Control Building in Fig. 1 along a tangent to the exit of Turn 16. Contact of right runner (left as viewed) with the inner wall lasts considerably less than 0.1 s (Photos captured by Les Schaffer.)

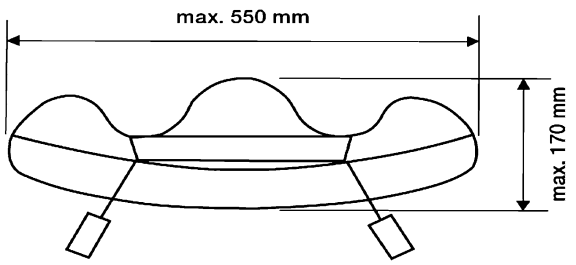

Fig. 3 Front view of a luge sled [7]. According to section 1.4 of FIL rules [7], the distance between the inner edges of the runners (here shown schematically relatively close together) must not exceed 0.450 m at any point and the maximum width of the sled, including shell and handles, must not exceed 0.550 m. See also Fig. 2

outer edges of the steels, on which the runners are mounted, are allowed to be almost as wide as the seat pod. This allows the runners to extend laterally far enough to contact the fillet at the base of the inner wall (Fig. 2).

2.2 Ice track description

Ice tracks are specific to the hill on which they are constructed. A particular track centerline profile is laid out on the chosen hill to have the correct average slope to give the gradual buildup and maintenance of speed desired. Tracks consist of straight segments connected by strongly banked curves (see Fig. 1). In straight segments the track cross section is rectangular and consists of two exactly vertical walls separated by a downward sloping, but flat, bottom or floor about 1.5 m wide. In curves the cross sections are shaped to contribute a horizontal component of the normal force sufficient to provide the centripetal acceleration toward the turn center needed to change the direction of the velocity vector. A typical banked cross section nearer the middle of a curve at the Calgary track is shown in Fig. 4a. As the sled nears the exit of the curve the cross section becomes closer to the shape shown in Fig. 4b, and the transition begins to the exactly rectangular cross sectional shape of the next straight segment. The inside walls of the banked sections in curves are also nearly vertical (Fig. 4a, b) and are adequately approximated locally as surfaces of right circular cylinders.

Because vehicle transitions from the curved into the straight segments of the track are not always centered and/or parallel to the center line, the vertical walls in the straight segments are joined to the flat bottom with a small radius (0.125 m) concave ice fillet, described as a "bottom inside corner ...[with] a rounded profile" in [2]. Indeed this fillet is required in section 16.14, Straights of the International Bobsled Federation (FIBT) rules [8] which states that "The transition between the sidewall and the base of the track must be provided with a channel [what is referred to here as a fillet]. In the iced state its radius must be

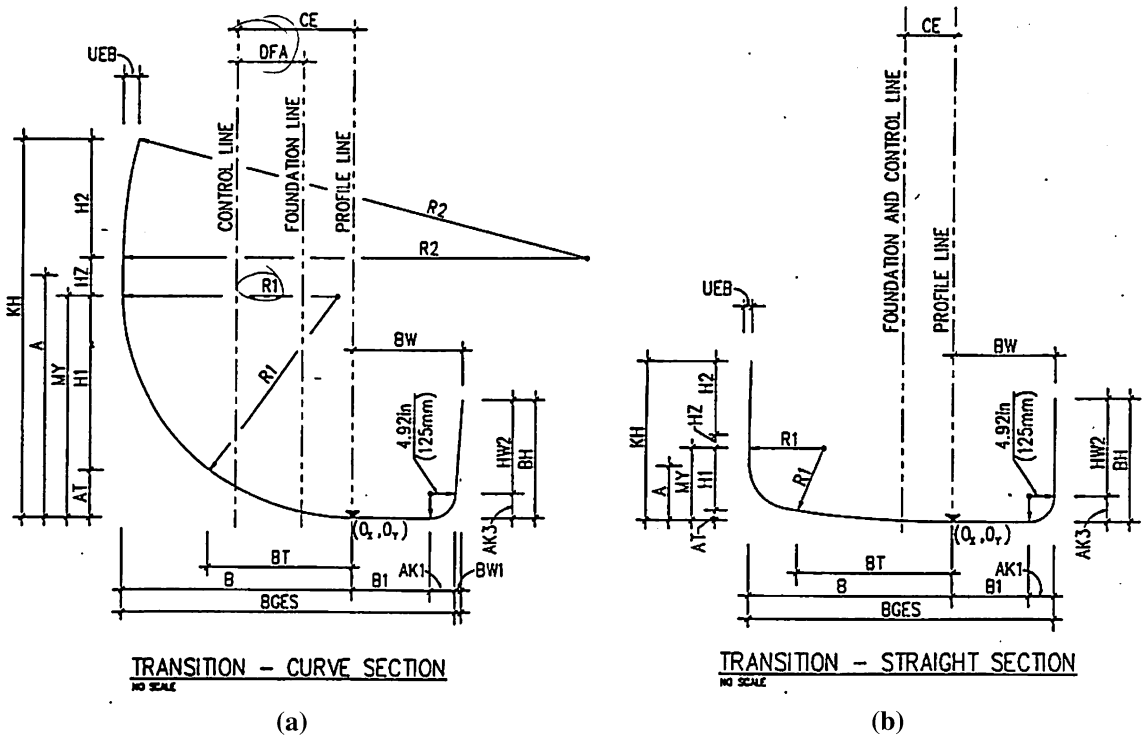

Fig. 4 Ice track cross sections are strongly banked in turns and roughly rectangular in straight segments. Shown here are two example cross sections from a banked turn on the Calgary track; **a** near the middle of the turn, and **b** near the turn exit where the cross section has become nearly rectangular. Both the curved and nearly straight cross sections contain a small radius ($r = 125$ mm) concave fillet at the lower right corner connecting the flat bottom to the right (looking down-track) inside vertical side wall. Seven of the last 8 Olympic tracks have been created by the same design firm, IBG of Leipzig, Germany and each has this design feature

10 cm." Presumably this fillet allows bobsled (and luge) runners to gently interact with the fillet, providing a centering action in the otherwise flat straight segments.

Although the rules justify the existence of the fillet in straights, the author is unaware of any such justification for their use at the base of inner walls in curved segments. Section 16.11, Bends of the FIBT rules [8] is notable for the absence of a similar specification. Nevertheless the fillet is also included in the design drawings of banked cross sections (Fig. 4a, b) connecting the inner wall to the floor. This fillet is even apparent in Fig. 2, the shape made plainly visible there by shadows.

2.3 Toroidal fillet geometry

At a point on the track where the track centerline slope β is zero (as is the case in Turn 16), the surface of the fillet itself can be approximated by the lower, inner one fourth of a large aspect ratio $\alpha = R/r$ torus with major radius R roughly equal to the turn radius, and minor radius r equal to the fillet radius. At a more general location where β is not zero a helical tube would be required, with the tube tilted in general from vertical through the average track slope at the particular location to allow connection with the gradually sloping floor.

The geometry of the torus is generally described parametrically in a coordinate system with origin at its center. Consider a similar $x_1y_1z_1$ coordinate system with origin O_1 on a vertical axis at the center of the turn, z_1 vertical, the y_1 axis toward the banked track surface, but with O_1 translated downward from the torus center along z_1 by r so that the y_1 axis passes through the point O of first contact of the particle sled with the bottom of the fillet. The equation of a local approximation of the cylindrical inner wall in this $x_1y_1z_1$ system is

$$x_1^2 + y_1^2 = (R - r)^2. \tag{1}$$

where R and r are the major and minor torus radii, respectively, and the location of point O in this coordinate system is (0, R, 0).

Now define the primary coordinate system xyz with origin at O as a rotation of system $x_1y_1z_1$ about y_1 through angle β, the slope of the floor relative to horizontal, followed by a translation of R along y_1 so that x is tangent, and z is perpendicular, to the generally sloping helicoidal floor at point O. The position vector $\mathbf{r}$ from O to a general point P on the toroidal approximation of the fillet in the xyz system is written as

$$\mathbf{r} = (x, y, z) \tag{2}$$

where it is assumed the difference between the position vector $\mathbf{r}$ and scalar minor torus radius r is clear from context.

Parametrically the coordinates of a point P on the surface can be written as

$$\begin{aligned} x(u,v) &= (R - r\sin v)\sin u \\ y(u,v) &= R(\cos u - 1) - r\sin v\cos u \\ z(u,v) &= r(1-\cos v) \end{aligned} \tag{3}$$

where the parameters u and v are angles along- and cross-track measured, respectively, about z_1 at the turn center and about the axis of the toroidal tube. Parameter v is the angle between the vertical and the line in a vertical plane perpendicular to the circular tube centerline from a point C on the tube centerline to the point P (v is zero when P is directly below C). Intuitively the angles u and v are the "longitude" and "latitude" of P, respectively, and the entire fillet ice surface lies in the range $0 < v < \pi/2$. Equations 3 make it clear that the position vector to an arbitrary point on the torus is a function $\mathbf{r} = \mathbf{r}(u,v)$ only of the two angles that parameterize the fillet surface [9].

2.4 Equations of motion on the fillet

Even though Fig. 2 shows clearly that there were two points of contact of the sled with the ice during the critical period of the accident, it is not necessary to invoke a two-point contact model to understand the essential mechanism of the sled interaction with the ice fillet surface. The simplest model with the ability to produce descriptive results is a particle model in which a point mass slides along the surface [10]. Models like this have been used previously to describe the dynamic motion of bobsleds on similar ice tracks [10, 11, 12]. And the recently completed independent audit of the Whistler track [4] used an identical particle model for simulations of sled trajectories.

Appendix A discusses the geometry of the toroidal fillet surface and presents the two equations of motion (coupled second order ordinary differential equations for the two parameters u and v) of a particle sliding on the surface. Although the differential geometry of the surface is developed there in more detail and emphasized because of its importance in the launch process, the equations of motion are essentially identical to those used in [10] to study the motion of the bobsled on ice tracks. These describe how u and v must change in accordance with Newton's laws.

3 Results

The equations of motion (Eq. 23) were used to study the interaction of the sled with the fillet surface. A MATLAB simulation program was created to solve the initial value problem to calculate $u(t)$ and $v(t)$ from the initial conditions at point O, the point of first contact with the fillet where $u(0) = v(0) = 0$, with initial speed s_o = 39.81 m/s, and with the horizontal velocity vector at a variable *entry angle* γ_o relative to the x axis tangent to the edge of the fillet toe. Thus the velocity initial conditions are $\dot{x}(0) = s_o\cos\gamma_o$ and $\dot{y}(0) = -s_o\sin\gamma_o$ which correspond to initial conditions for the speed parameters $\dot{u}(0) = s_o\cos\gamma_o/R$ and $\dot{v}(0) = s_o\sin\gamma_o/r$.

Physical and track geometric parameters used are shown in Table 1. The combined slider and luge mass m is realistic, but the dynamic equations of motion Eq. 23 are mass independent (see Appendix A). Thus a precise value of m is not important. Present day track centerline layout designs use clothoid curves that linearly vary the track centerline curvature to smooth transitions at inlets to and outlets from curves. So even though the minimum radius of curvature in Turn 16 is about 33 m, at the location of the inner wall collision R was closer to 38 m as measured from track overhead views. Because the accident occurred at the very bottom of the track near where the average 0.105 downgrade reverts to an uphill one to assist in sled deceleration, it is assumed that the centerline slope $\beta = 0$. Although the speed in the Whistler accident was measured to 1 mm/s in real time, the top speed during qualifying was at least 154.0 km/h (42.78 m/s) [2] and this speed should be used in further safety predictions for this track. The exact value of h_w is also not too important since, as will be shown below, the height achieved in flight h_z is a linearly increasing function of the angle γ_o at which entry to the fillet occurs.

Considerable effort was made by this author (see Sect. 4 below) to obtain more precise values for certain parameters (R, r, h_w and β) in Table 1 but this attempt was

Table 1 Physical and geometric parameters

Parameter	Symbol	Value	Units
Acceleration of gravity	g	9.81	m/s^2
Mass of slider, ballast and sled	m	110[a]	kg
Turn wall radius at fillet contact	R	38[b]	m
Fillet radius	r	0.125[c]	m
Centerline slope	β	0[d]	rad
Initial speed	s_o	39.8	m/s
Exit outside wall height	h_w	1.0[e]	m
Diagonal cross-track distance	d	23.4[f]	m

[a] Estimated [7]

[b] Measured from Googlemaps

[c] See Fig. 4a

[d] Estimated

[e] Estimated from photographs

[f] Measured from Googlemaps

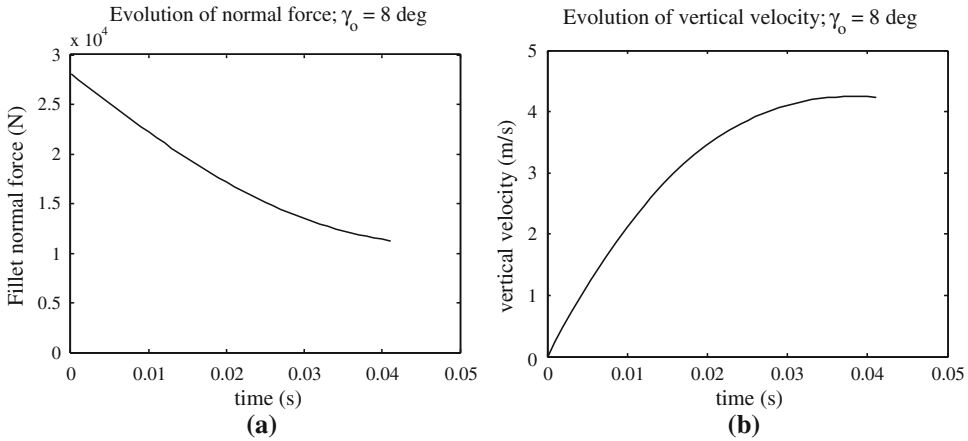

Fig. 5 Simulation results for entry angle $\gamma_o = 8°$. Contact duration is only 0.041 s but contact persists until the top of the fillet is reached. **a** Normal force decreases from 28 to 11 KN, and the average force of 14 KN during the last half of contact acts nearly horizontally. **b** A substantial portion (>80 %) of the vertical velocity at launch is achieved in less than half the contact time because the normal force acts mostly in the vertical direction during this period

unsuccessful. The author believes that, while more accurate values of these parameters are somewhat desirable, additional accuracy would add very little to the conclusions of this study, and that certainly the unwillingness of the authorities to provide these should not be allowed to prevent or further delay the analysis.

Results from a simulation with $\gamma_o = 8°$ (0.14 rad) (chosen as an illustrative example) are presented in Figs. 5 and 6. Total contact duration is very short, $t_c = 0.041$ s. Although not shown, fillet latitude rises almost linearly in time, reaching a value of $\pi/2$ at $t = t_c$. Figure 5a portrays the evolution of the normal force as a function of time. Because of the discontinuity in normal curvature (see Appendix A) between the flat floor ($\kappa_n = 0$) and the fillet, the normal force rises discontinuously at $t = 0$ by roughly a factor of 25 from the weight $mg = 1079$ N to about 28 KN. During the entire contact period the normal curvature in the direction of the path is positive in the sense that, along the path, the fillet surface is "rising" to meet the velocity vector. When the luge reaches the top of the fillet ($z = 0.125$ m) at its junction with the cylindrical inner wall, however, the wall surface normal curvature becomes negative (the two principal curvatures for a cylinder (see Appendix A) are $\kappa_1 = 0$ m^{-1} and $\kappa_2 = -1/(R - r)$ m^{-1}). Contact is lost (the sled and slider are launched) because there is no component of the weight perpendicular to the vertical surface to supply the needed normal acceleration and maintain contact. The normal force decreases by more than half during the contact period but is still very large (11.5 KN) just before contact ends.

A large fraction of the vertical speed at launch s_{lz} of 4.24 m/s is generated during the first 0.02 s of contact (Fig. 5b). This vertical velocity results in a peak (zenith) height h_z of the center of mass in subsequent free flight of

$$h_z = 0.125 + s_{lz}^2/2g. \tag{4}$$

For this example $h_z = 1.04$ m, as high as or higher than the estimate of the retaining wall height h_w at the curve exit.

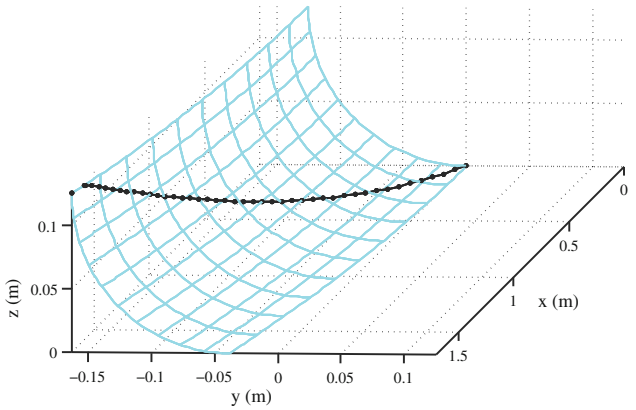

Fig. 6 Simulation results (x axis not to scale) for entry angle $\gamma_o = 8°$. Luge 3D path rises to top of fillet as inner wall turns away from initial direction. Loss of contact occurs when the positive normal curvature at the top of the fillet vanishes where it meets the cylindrical inner wall

Larger entry angles γ_o result in even larger vertical velocities when wall contact ends and correspondingly larger zenith heights.

The corresponding three dimensional path on the fillet surface is portrayed in Fig. 6. Fillet contact occurs only over a relatively short length ($\simeq 1.546$ m) of track. Because, as the sled rises on the fillet, the surface itself is turning away from the down track direction, not all the initial lateral (y) velocity $s_o \sin\gamma_o$ can be turned (literally) into vertical velocity s_{lz}, as is shown in more detail below.

Contained in Fig. 7 is a summary of the simulated ejection flight path resulting from fillet entry angle $\gamma_o = 8°$ at initial speed $s_o = 39.81$ m/s and neglecting aerodynamic forces. The slider path (red) on the fillet ice surface (the ice fillet patch is also shown) is identical to that in Fig. 6, but is here shown at the base of the curved inner wall. Loss of ice contact occurs at the fillet-wall boundary at $x = 1.54$ m. Thereafter, the flight path rises and barely clears the outer wall at the red dot. The vertical plane containing the flight path (shown in black with projections down to the ice floor) is tangent to the curving cylindrical inner wall at the (single

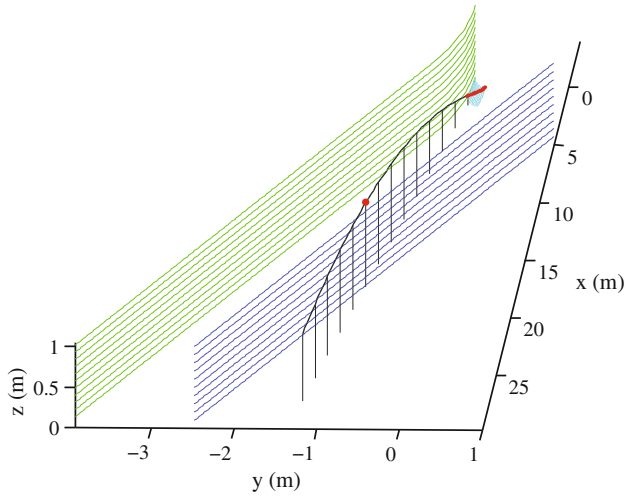

Fig. 7 Schematic of ejection flight path resulting from fillet entry angle $\gamma_o = 8°$ at initial speed $s_o = 39.81$ m/s. Path (*red*) on the fillet ice surface (ice fillet patch shown in *cyan*) is identical to that in Fig. 6. Here it is shown at the base of the curved (*green*) inner wall. Loss of ice contact occurs at $x = 1.54$ m. Thereafter, flight path (*black*) rises and barely clears outer (*blue*) wall at *red dot*. *Note x* axis not to scale

and last) point of contact of the ice path with the inner wall. Because the inner wall is not yet straight, this vertical plane makes nonzero angle with the straight outer wall and the flight path will either collide with the vertical surface of the outer wall or clear it as shown in Fig. 7, depending on the magnitude of the vertical velocity at launch. Note that the x axis in Fig. 7 is not to scale.

Figure 8 shows a summary of results of 100 such simulations for entry angles in the range $0 < \gamma_o < 10°$. Three regions of distinct behavior occur (see Fig. 8a, d). For small entry angles $0 < \gamma_o < 2.35°$, duration of fillet contact rises linearly (Fig. 8d) from 0 to $t_c = 0.075$ s but, because the normal curvature is small even though it is negative, the gravity force is sufficient to hold the sled down on the nearly horizontal fillet surface and to maintain contact. The sled rejoins the floor when $v(t_c) = 0$, simply riding over the low "toe" of the fillet. For $2.35 < \gamma_o < 6.2°$ the negative normal curvature and corresponding normal acceleration at the maximum value of fillet "latitude" v are too large to be supplied by the gravity force and contact is lost at increasing values of v (Fig. 8a) as contact time gradually increases (Fig. 8d) from 0.030 to 0.063 s. For $\gamma_o > 6.2°$, contact persists all the way to the top of the fillet where $v_{\max} = \pi/2$, but contact time gradually decreases again to 0.031 s when $\gamma_o = 10°$.

The vertical component of velocity at loss of contact s_{lz} (Fig. 8b) rises more and more rapidly with increases in γ_o and becomes a larger percentage of the lateral entry speed. When $\gamma_o = 8°$ the vertical velocity is 4.24 m/s leading to a zenith height of the resulting ballistic ejection trajectory of 1.04 m. Zenith height is extremely sensitive to entry angle.

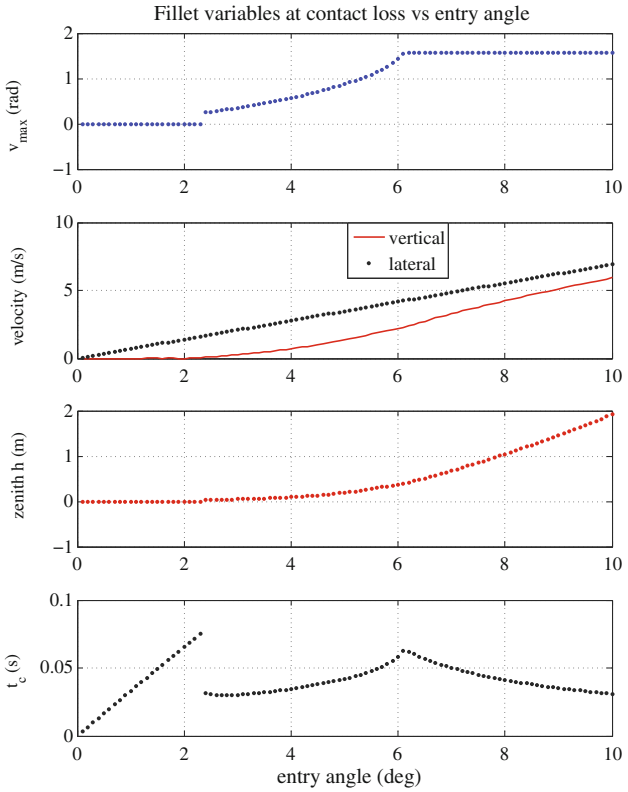

Fig. 8 Fillet interaction variables vs. entry angle γ_o at constant initial speed $s_o = 39.81$ m/s: **a** fillet latitude $v_{\max}$ at loss of contact, **b** lateral entry speed s_{oy} and vertical velocity at loss of contact s_{lz}, **c** zenith height of resulting ballistic path, **d** fillet contact time. Three regions of distinct behavior exist depending on entry angle. For $\gamma_o > 6.2°$ contact persists continuously to top of fillet ($v_{\max} = \pi/2$). As entry angle approaches $\gamma_o = 10°$ almost all lateral entry velocity is converted to vertical ejection velocity and zenith height h_z of the subsequent flight trajectory after launch approaches 2 m. Distance to subsequent flight zenith is roughly initial speed s_o times vertical launch velocity s_{lz} divided by g

Increasing γ_o from 8° to 10° doubles the zenith height (Fig. 8c) of the flight path!

The zenith occurs at a substantial distance d_z from the point of loss of contact. Because the vertical component of velocity 4.24 m/s decreases the horizontal component only slightly more than 1 %, the horizontal distance d_z to the zenith position is given approximately by

$$d_z = s_o t_f = s_o s_{lz}/g \tag{5}$$

where t_f is the time of flight to the zenith. At a given entry speed s_o, both t_f and d_z vary roughly linearly with entry angle γ_o, but for fixed entry angle γ_o, d_z varies approximately quadratically with initial speed s_o, as does h_z. Timing is important. For the example shown in Figs. 5 and 6, ($\gamma_o = 8°$), zenith height occurs at $t_f = 0.43$ s and $d_z = 17$ m. This is not far from the estimated diagonal cross track distance d (see Table 1) from the point of loss of inner wall contact to the exit wall.

4 Discussion

4.1 Effect of fillet on track ejection

When the particle sled encounters the fillet at a non-zero entry angle γ_o, the lateral y component of horizontal velocity $s_{oy} = s_o \sin\gamma_o$ causes motion of the sled in the v direction up the fillet. The fillet normal force resulting from its strong positive curvature acts perpendicular to this lateral velocity to turn it gradually upward while contact persists. If the inner wall were not curved but rather straight (as it is in straight segments), when the top of the fillet is reached the initially lateral component of velocity would be transformed to vertical velocity of essentially the same magnitude. The toroidal fillet acts less strongly (Fig. 8b) because its surface is continuously turning away from its initial direction, but it still is capable of generating vertical velocities and eventual free flight zenith heights larger than the outside exit wall heights that should be intended and designed to contain the slider.

It is a legitimate concern that the mass model used above is a particle while the actual slider and sled have mass distributed over a lateral distance of the order of 0.5 m (remember that the sled is restricted by rules [7] to a maximum width of 0.55 m). Another complication is that that the sled and slider composite body is not rigid but rather two bodies that can move relative to one another and can (and did) separate. Thus the results in Sect. 3 must be interpreted with care. Were the slider rigidly affixed to the sled then it is clear that an entry angle not much larger than $\gamma_o = 10°$ would cause a vertical velocity of the right runner of substantially more than 6 m/s (Fig. 8b) and that roughly half of this would be contributed to the center of mass (c.m.), sufficient for ejection.

As the sled rides up the fillet, the horizontal component of the normal force increases and the sled lateral velocity decreases. Because the slider's body continues toward the wall over the right runner (Fig. 2b, c), his displaced c.m. will receive more than half the velocity of the runner, so that an estimate for the required entry angle for ejection of $\gamma_o > 11°$ is probably not far off. It is also worth noting that the large horizontal component of the normal force acting on the front half of the sled late during contact accounts for the rotation, after loss of contact, of the slider and sled about the vertical axis in the direction observed in Fig. 2c, d, e.

It is essential to comment on the importance of the negative Gaussian curvature, i.e. the fillet at the base of an inside wall (see Appendix A), on the capacity for ejection. The positive lateral normal curvature of the fillet that was designed into it, $\kappa_2 = 1/r$, gives it the capacity to turn the lateral component of incident velocity to a vertical one. The negative longitudinal normal curvature of the fillet $\kappa_1 = -\sin v/(R - r\sin v)$ and that of the cylindrical wall above it cause contact with the fillet or inner wall eventually to be lost at high speeds and large entry angles. Thereafter the subsequent center of mass flight path lies in a vertical plane nearly tangent to the curving inner wall at the launch point, with the near inner wall turning away from it and only the outside wall remaining to contain the slider in flight. This vertical plane intersects the outer wall and thus the slider path can pass over the outer wall if it is not high enough (Fig. 7). The simulations above show that there exists an entry angle γ_o that causes vertical launch velocity more than sufficient to clear the roughly 1 m outside wall that was present.

Crucial structural components of luge sleds are two bridges [7], essentially inverted-U-shaped symmetric steel beams (with approximate depth $\simeq$6 mm and width $\simeq$50 mm), that originate and terminate in the left and right runners, respectively, and pass through and support the sled body. The normal force as a function of time in the example calculations (Fig. 5a) explains not only the vertical velocity required for ejection but also the deformation of the right sled runner and bridge observable in Fig. 2d, e, and claimed by the FIL Official Report [1] to be the cause of ejection. An analysis of the bridge (not included here) shows that bending deformations of this magnitude are reasonable given the magnitude ($\simeq$14 KN) of the average normal force later during contact. It also shows that early in contact the direction of the normal force was more nearly aligned with the lower part of the bridge near the runner contact point causing mostly axial compression along the bridge rather than bending. But the bridges are designed to bear loads in this direction. Only later during the contact period is the normal force in a direction to effectively cause bending. By this point most of the vertical velocity required for ejection has been attained (Fig. 5b).

Furthermore the catapulting (whatever this means precisely), if any occurred, happened late in the contact period when the result of catapulting would have been largely horizontal rather than vertical. By the time the normal force has the direction relative to the sled that is required for bending the bridge, the vertical velocity has largely been acquired. Catapulting did not produce the vertical velocity of ejection. Rather the vertical velocity of ejection is entirely accounted for by the very large vertical normal force early in the contact period due to the circular shape of the fillet on the inside wall.

The results above point incontrovertibly to the shape of the fillet as the proximate cause of ejection of Nodar Kumaritashvili from the Whistler Track. Contrary to the FIL report [1] that the cause of the accident was a mysterious "catapult effect", the sled was merely sliding on the ice surface in a way that was entirely predictable. The ice

surface simply had the wrong shape and it was the interaction of the right runner with the fillet shape that caused a vertical velocity more than adequate to clear the exit wall. *A fillet at the base of an inside wall can launch the slider into flight across the track.*

If the fillet had not been present, and instead the inner wall and floor had intersected at a right angle, the slider would have collided with the cylindrical wall with a horizontal lateral velocity of perhaps 4–7 m/s (corresponding to an equivalent fall height of 0.8–2.5 m) onto the wall ice surface. The slider might have been severely bruised but would most likely still be alive. Flight sufficient to result in ejection would almost certainly not have occurred because the impulses from the cylindrical wall and the corresponding post-impact velocity would have been essentially horizontal.

Yet track ejection consists of two essential components: (1) generation of velocity at loss of wall contact with magnitude and direction sufficient to result in flight, and (2) a failure to contain the resulting flight trajectory, if it occurs, with sufficiently confining walls. Once flight takes place the surrounding safety surfaces must enclose the trajectory so that re-entry from flight to sliding again occurs as a result of collision at low incidence angles with smooth, low-friction ice surfaces rather than at high angles with immovable fixed objects outside the enclosed tube.

Safe design consists of first ensuring that no flight takes place, and secondly (even if the first goal is not achieved) that the path does not pass above and outside the enclosing walls. The Whistler track failed in both respects. In no case should a driving error by a slider have fatal consequences. As eloquently stated by Georgian President Mikahail Saakshvili, "No sports mistake is supposed to lead to a human death." Safe ice track design encompassing the above two aspects ensures this.

It has been widely reported that the top speeds measured at the track are considerably (about 13%) larger than the design values. Although the final design document "specified a maximum pre-calculated speed of 136.3 km/h [37.86 m/s]" [2], by 2009 "speeds of 154 km/h [42.78 m/s] had been reached," ... showing "that the designer's calculations of top speeds were incorrect." [2]. The Coroner's report [2] also describes fairly completely the history of the design process, the concerns of the FIBT and FIL, and the evolution of the realization of the excess speed problem. All other things (track shape and entry angle in the collision) being equal, the lateral velocity is directly proportional to slider speed. A 13 % increase in total speed leads to a 13 % increase in lateral velocity, roughly a 13 % increase in vertical velocity at launch, and a 27 % increase in peak height of the ballistic trajectory due to the vertical velocity. Thus, all other things being equal, if the slider had been on a slower track traveling at a fractional speed 1/1.13 = 0.89 of the excessive speeds achieved on the Whistler track, his peak height would have been reduced by a factor of 1/1.27= 0.78 ((Fig. 8b) and he would have likely hit the inside top of the wall and been retained, rather than narrowly clearing it resulting in ejection. One wonders whether the clearly perceived excess speed affected any design decisions, especially modification of exit wall heights as the design and speeds evolved before the accident.

The recently released independent, and ostensibly comprehensive, safety audit of the track [4] recommended by the Coroner's report [2] relied on a particle model identical to that used herein. It vaguely alluded to, but failed to identify, the cause of the Kumaritashvili accident. Two of its more interesting and striking conclusions were that: (1) "In C16 careful consideration must be given to the ice profile between the track floor and the right wall on the exit of C16. Oversized rounded fillets between the floor and the right wall could, in effect, create a ramp upon which the right runner of the luge could ride up." [4] (p. 256), and (2) "All entry lines into C16, if left to run freely, appear to result in an impact on the right side of the track on exit." [4, p. 251]!

4.2 Limitations of the particle model

Deformation of the slider's body and compression into the sled are neglected in the sliding particle model discussed here. Furthermore, the slider and sled are assumed to be *one* body and to not separate. Deformation, to the extent that it occurs, will dissipate energy and the restitution of compression will also cause separation once mutual flight begins. For these reasons the sliding particle model is completely predictive only during the period when the bodies remain together. It cannot be expected to predict the separate phenomena of deformation and separation. In passing, one consequence of compression is that the flight trajectories of the sled and slider separate from one another, the slider being pushed even higher and the sled even lower than the path of the common center of mass of the slider and sled together. In this sense the predictions of slider zenith height as a function of entry angle are conservative.

In spite of these limitations, the particle model is able to predict the first order properties (the essence) of the launch phenomenon and its use is entirely appropriate for the study of launch and ejection. Although the recently completed independent audit of the Whistler track [4] failed to identify the cause of slider ejection in the Kumaritashvili accident, it used precisely the same model as the one in this paper.

The estimates above of the normal force (Fig. 5a) should be viewed as upper bounds since deformation of the slider's body will decrease these somewhat. Nevertheless,

even though the predicted normal force is large (e.g. a 20 KN force applied directly to any single bone may be sufficient to cause its failure), it should be emphasized that the normal force is spread over the entire surface of the slider's back. Viewed in this way a 20 KN force distributed over, say, an area of 0.1 m^2 results in only a fairly modest pressure of roughly 200000 Pa = 2 atm. It is perhaps surprising that such a small pressure acting over such a short time can result in slider ejection.

4.3 Efficacy and transparency of the review and investigation process

Requests to both the designer and Whistler Sport Legacies Society (WSLS) authorities to provide precise values for only four geometric track parameters contained in Table 1 were unsuccessful. The designer's response to the initial request was that official approval was required from Whistler Sport Legacies Society, the present track owner. Numerous email and other messages over a period of six months to the WSLS authorities elicited generally positive assurances that the requested information could be made available, but nothing was ever provided. New ice tracks are built every 4 years like clockwork, and they involve very large sums of public money (the Whistler track cost C$105M). The entire design process needs to be made more transparent and open, with the possibility of independent, financially disinterested, scientifically competent individuals involved at every stage. Details of the track design should be available to interested parties for the purpose of independent review and investigation rather than being guarded in a process that is as secret and closed as at present. Even the recently concluded and published independent audit of track safety [4] is subject to confidentiality agreements and no public disclosure by the authors is permitted without the explicit consent of WSLS [3] .

5 Summary and conclusions

This rudimentary study has made clear how ice track ejection can be explained with a simple analytic model of fillet surface shape and an equally simple model of dynamics on this surface based on Newton's laws. Yet it raises more questions than it answers. Some of these are: (1) Why is the fillet present in design specifications and drawings of curved inner wall shape designs when it is not required or even mentioned in the rules? What, if any, is its role perceived to be by the designers? (2) Why, even if included at the base of the inner wall, was the specified value 0.125 m of fillet radius r different from the only value of r, 0.1 m, mentioned in the rules? (3) Were the exit wall heights adjusted throughout the evolution of the design after the actual track speeds were realized to be larger than expected? If so, how? (4) According to the FIL report, the "existing safety wall, ... had already been lengthened and raised in the area of the accident," [1]. On what basis was the height of wall calculated? (5) Why is the design process not more open and transparent, and more able to rely on the well-meaning scrutiny of interested but financially non-conflicted scientists and engineers around the world?

The main conclusions of this paper are:

1. The interaction of the right runner with the fillet at the bottom of the inner wall resulted in the vertical velocity necessary for, and thus was the cause of, the ejection of Nodar Kumaritashvili from the track in the Vancouver Olympic luge accident.
2. The presence of fillets at the base of inner walls of curves is an ice track design flaw that exposes sliders to ejection. These are neither required by nor even mentioned in the Federation Rules and absolutely should be prohibited in future designs. Furthermore these should be removed from the base of inner walls in all turns at the Whistler track and other existing tracks.
3. The bending of the bridge was certainly caused by the normal force from the fillet but this occurred mostly during the last half of the contact period when the normal force was largely horizontal and thus its rebound was not able to provide vertical impulse. The bending of the bridge was not the cause of ejection.
4. A more open review and investigation process is highly desirable and could only increase the resulting safety of athletes using the tracks.

One is left to ponder why it has taken nearly three years to explain fully the cause of the accident, especially when the very day after it occurred the offending fillet was removed entirely from the track [1] as quoted in the second paragraph of this paper. Even the recently released independent and impartial safety audit [4] has not done this. The present paper is the first to follow the implications of Newton's laws to their logical conclusion: there must have been some cause of the vertical velocity required for ejection. This cause must have been a very large force with a large impulse acting in the vertical direction. Only the interaction of the runner with the fillet could have provided it.

Acknowledgments The author gratefully acknowledges ongoing discussions regarding the video footage with Andy Ruina and Les Schaffer during the ten days after the accident. These were valuable in clarifying the sequence of events and the facts of the accident itself. Also acknowledged are helpful discussions with and suggestions from Lyn Taylor, Michael Drapack, Frank Masley, Jeff Kluewer, and Steve Tracy.

Appendix A

We begin with an analytic approximation for the toroidal fillet surface connecting the cylindrical inner wall and the planar floor and then present the equations of motion for a particle travelling on this specific surface, based on equations for motion of a particle on a general 2-D surface [10].

Toroidal fillet geometry

At the location of the Olympic accident the track slope $\beta = 0$ and the fillet surface is well approximated by a torus (Theory similar to that presented in this paper can be used in the more general situation where $\beta \neq 0$ and the fillet shape is a helical tube rather than a torus). When the floor slope angle $\beta = 0$, the implicit equation of the torus is

$$(R - \sqrt{x^2 + y^2})^2 + z^2 = r^2. \tag{6}$$

The xyz coordinates of a point on the fillet are given by

$$\begin{aligned} x(u,v) &= (R - r\sin v)\sin u \\ y(u,v) &= R(\cos u - 1) - r\sin v\cos u \\ z(u,v) &= r(1 - \cos v) \end{aligned} \tag{7}$$

Equations 7 emphasize that the position vector to an arbitrary point on the torus is a function $\mathbf{r} = \mathbf{r}(u,v)$ of the two surface (angle) parameters u and v [9]. The terminology of Faux and Pratt [9] is followed closely here.

The velocity vector lies along a tangent to the surface

$$\mathbf{v} = \dot{\mathbf{r}} = \mathbf{A}\dot{\mathbf{u}} \tag{8}$$

where

$$\mathbf{A} = \begin{bmatrix} \dfrac{\partial \mathbf{r}}{\partial u} & \dfrac{\partial \mathbf{r}}{\partial v} \end{bmatrix} \tag{9}$$

and

$$\dot{\mathbf{u}} = \begin{bmatrix} \dot{u} \\ \dot{v} \end{bmatrix}. \tag{10}$$

The analytic expression for the torus surface makes it possible to compute analytically its partial derivatives with respect to u and v. Specifically,

$$\frac{\partial \mathbf{r}}{\partial u} = \begin{bmatrix} (R - r\sin v)\cos u \\ -(R - r\sin v)\sin u \\ 0 \end{bmatrix}, \tag{11}$$

$$\frac{\partial \mathbf{r}}{\partial v} = \begin{bmatrix} -r\sin u\cos v \\ -r\cos u\cos v \\ r\sin v \end{bmatrix}, \tag{12}$$

$$\frac{\partial^2 \mathbf{r}}{\partial u^2} = \begin{bmatrix} -(R - r\sin v)\sin u \\ -(R - r\sin v)\cos u \\ 0 \end{bmatrix}, \tag{13}$$

$$\frac{\partial^2 \mathbf{r}}{\partial v^2} = \begin{bmatrix} r\sin u\sin v \\ r\cos u\sin v \\ r\cos v \end{bmatrix}, \tag{14}$$

and

$$\frac{\partial^2 \mathbf{r}}{\partial u \partial v} = \frac{\partial^2 \mathbf{r}}{\partial v \partial u} = \begin{bmatrix} -r\cos u\cos v \\ r\sin u\cos v \\ 0 \end{bmatrix}. \tag{15}$$

The first and second fundamental matrices $\mathbf{G}$ and $\mathbf{D}$ of the toroidal surface are functions of the partial derivatives above:

$$\begin{aligned} \mathbf{G} = \mathbf{A}^{\mathrm{T}}\mathbf{A} &= \begin{bmatrix} \dfrac{\partial \mathbf{r}}{\partial u}\cdot\dfrac{\partial \mathbf{r}}{\partial u} & \dfrac{\partial \mathbf{r}}{\partial u}\cdot\dfrac{\partial \mathbf{r}}{\partial v} \\ \dfrac{\partial \mathbf{r}}{\partial v}\cdot\dfrac{\partial \mathbf{r}}{\partial u} & \dfrac{\partial \mathbf{r}}{\partial v}\cdot\dfrac{\partial \mathbf{r}}{\partial v} \end{bmatrix} \\ &= \begin{bmatrix} (R - r\sin v)^2 & 0 \\ 0 & r^2 \end{bmatrix} \end{aligned} \tag{16}$$

and

$$\begin{aligned} \mathbf{D} &= \begin{bmatrix} \mathbf{n}\cdot\dfrac{\partial^2 \mathbf{r}}{\partial u^2} & \mathbf{n}\cdot\dfrac{\partial^2 \mathbf{r}}{\partial u \partial v} \\ \mathbf{n}\cdot\dfrac{\partial^2 \mathbf{r}}{\partial v \partial u} & \mathbf{n}\cdot\dfrac{\partial^2 \mathbf{r}}{\partial v^2} \end{bmatrix} \\ &= \begin{bmatrix} -(R - r\sin v)\sin v & 0 \\ 0 & r \end{bmatrix} \end{aligned} \tag{17}$$

and where the unit surface normal $\mathbf{n}$ is given by

$$\mathbf{n} = -\left(\frac{\partial \mathbf{r}}{\partial u} \times \frac{\partial \mathbf{r}}{\partial v}\right) \Big/ \left|\frac{\partial \mathbf{r}}{\partial u} \times \frac{\partial \mathbf{r}}{\partial v}\right| = \begin{bmatrix} \sin v\sin u \\ \sin v\cos u \\ \cos v \end{bmatrix}. \tag{18}$$

The negative sign in Eq. 18 is chosen so that $\mathbf{n}$ points away from the ice surface and into the track (and the torus) interior.

The normal curvature κ_n of the torus in the tangent direction $\mathbf{v} = \mathbf{A}\dot{\mathbf{u}}$ is defined as the curvature of the curve of intersection of the surface and the plane containing the tangent vector $\mathbf{v}$ and the surface normal $\mathbf{n}$ [9]. It is a ratio of quadratic forms in $\dot{\mathbf{u}}$ with the matrices $\mathbf{G}$ and $\mathbf{D}$ as coefficients [9]

$$\kappa_n = \frac{\dot{\mathbf{u}}^{\mathrm{T}}\mathbf{D}\dot{\mathbf{u}}}{\dot{\mathbf{u}}^{\mathrm{T}}\mathbf{G}\dot{\mathbf{u}}}. \tag{19}$$

The directions in the surface at the point (u, v) for which the normal curvature κ_n becomes a minimum and maximum are called the principal directions of normal curvature, and the corresponding normal curvatures κ_1 and κ_2 are called principal curvatures. The product of the principal curvatures, the Gaussian curvature K, is also related to matrices $\mathbf{G}$ and $\mathbf{D}$ through

$$K = \kappa_1 \kappa_2 = \frac{|\mathbf{D}|}{|\mathbf{G}|} = \frac{-\sin v}{r(R - r\sin v)}. \tag{20}$$

Due to symmetry, one of the principal curvatures of a torus is the inverse of the minor radius $\kappa_2 = 1/r$. Hence the other principal curvature is given by $\kappa_1 = -\sin v/(R - r\sin v)$, the negative sign indicating that along the (longitudinal) first principal direction in question, the surface "falls away" from the inward pointing normal vector $\mathbf{n}$.

Normal curvature at a specific point (u, v) varies continuously with direction ϕ according to Euler's formula [13]

$$\kappa_n(\phi) = \kappa_1 \cos^2\phi + \kappa_2 \sin^2\phi \tag{21}$$

where ϕ is the angle measured in the tangent plane about $\mathbf{n}$ from the first principal direction (of increasing "longitude") corresponding to curvature κ_1.

Because $R \gg r$, when the parameter $v > 0$ the Gaussian curvature is negative and there is a direction in the surface tangent plane at critical angle ϕ_c for which the normal curvature vanishes. This value of ϕ_c can then be calculated by substitution of $\kappa_n = 0$ into Eq. 21.

$$\phi_c = \arctan\sqrt{\frac{r\sin v}{R - r\sin v}}. \tag{22}$$

This direction separates those directions for which $\kappa_n > 0$ and surface contact is maintained at all speeds from those in which $\kappa_n < 0$ and loss of contact is possible at some speed.

Equations of motion

As the particle slides along the surface the parameters u and v and their derivatives change according to Newton's laws [10]. Here the generalized speeds [14] are chosen to be the angular rates $\dot{u}$ and $\dot{v}$, the two components of $\dot{\mathbf{u}}$.

Although in general motion of luge, bobsled and skeleton on ice tracks all forces (including weight, normal force, aerodynamic lift and drag, ice friction and steering forces) are important for accurate prediction [10], in the fillet contact problem considered here the surface normal force resulting from normal acceleration due to fillet curvature is enormous. Further, the aerodynamic and friction forces are typically an order of magnitude smaller than the weight, the coefficient of friction and drag area being of the order of 0.01 and 0.05 m^2, respectively [15, 16]. Thus only the first two of these forces, weight and normal force, are included in the present analysis; the former only to ascertain its role in delaying loss of surface contact, and the latter because the vertical component of its impulse causes the vertical velocity required for ejection.

Similar to the development in the Appendix of [10], the equations of motion for a particle sliding on the surface become

$$m\mathbf{G}\ddot{\mathbf{u}} = -m\begin{bmatrix} \frac{\partial \mathbf{r}}{\partial u}\cdot\mathbf{f_s} \\ \frac{\partial \mathbf{r}}{\partial v}\cdot\mathbf{f_s} \end{bmatrix} \tag{23}$$

where

$$\mathbf{f_s} = g\mathbf{k} + \frac{\partial^2 \mathbf{r}}{\partial u^2} + 2\frac{\partial^2 \mathbf{r}}{\partial u \partial v} + \frac{\partial^2 \mathbf{r}}{\partial v^2} \tag{24}$$

and where $\mathbf{k}$ denotes the unit vector in the vertical direction. Note that Eq. 23 is independent of mass since each term contains the factor m.

The normal force $\mathbf{N}$ is a constraint force that insures that the luge remains in contact with the ice surface (when the normal curvature is positive). $\mathbf{N}$ vanishes when the normal component of the weight mg is insufficient to supply the negative normal acceleration (associated with negative normal curvature) to maintain surface contact. Loss of surface contact is synonymous with $\mathbf{N}$ vanishing. When $\mathbf{N}$ is nonzero its magnitude is directly proportional to the mass and is given by

$$N = m\kappa_n|\mathbf{v}|^2 + mg\mathbf{n}\cdot\mathbf{k}. \tag{25}$$

The fillet and the inner wall surfaces are, generally speaking, the only portions of the entire ice surface for which there exist sliding directions in which the normal curvature is negative. Thus, assuming that the vertical component of the unit normal is positive (and the track surface doesn't go upside down) so that the gravity force acts to hold the slider on the surface, they are the only portions of the surface from which launch into flight can occur. To the extent that inner walls are vertical, sliding on these is impossible since they turn away from the interior (the normal curvature is always negative or zero) and launch always occurs instantaneously when contact occurs with an inner wall. The fillet, when it exists at the base of an inner wall, is the entrée to the wall and, even though contact and a positive normal force may persist throughout the entire sliding path on the fillet, the path eventually leads to the wall segment of the surface and certain launch. This is why the existence of a fillet at the base of an inner wall is a track design flaw.

References

1. International Luge Federation (2010) Official report to the International Olympic Committee on the accident of Georgian athlete, Nodar Kumaritashvili, at the Whistler Sliding Center, Canada, on February 12, 2010, during official luge training for

the XXI Olympic Winter Games. http://www.fibt.com/fileadmin/Rules/International_Rules_-_Bobsleigh_english_ver_1-1_16092007.pdf. Accessed Dec 2011
2. Pawlowski T (2010) Coroner's report into the death of Kumaritashvili, Nodar. British Columbia Ministry of Public Safety and Solicitor General. Case No: 2010-0269-0002
3. Whistler Sliding Center (2010) Request for expressions of interest for an evaluation of sled trajectories within the track of the Whistler Sliding Centre. 1 Dec 2010
4. Zahavich ATP, Bromley R, Montgomery J, Bernamann M, MacKenzie S, Cripton P (2012) Whistler Sliding Centre sled trajectory and track construction study: an independent safety audit as recommended by the BC coroner. http://www.whistlersportlegacies.com/reports/safetyaudit. Accessed Dec 2012
5. The New York Times (2010) Luge crash at the Olympics. http://www.nytimes.com/interactive/2010/02/12/sports/olympics/LUGEDEATH.html. Feb 2010
6. The Huffington Post (2010) Nodar Kumaritashvili crash VIDEO: luge slider DEAD in Olympics accident. http://www.huffingtonpost.com/2010/02/12/nodar-kumaritashvili-cras_n_460474.html. Feb 2010
7. International Luge Federation (2010) IRO International Luge regulations—artificial track. International Luge Federation
8. International Bobsleigh and Skeleton Federation (2007) International Rules, Bobsleigh. http://www.fibt.com/fileadmin/Rules/International_Rules_-_Bobsleigh_english_ver_1-1_16092007.pdf. Accessed Dec 2011
9. Faux ID, Pratt MJ (1979) Computational geometry for design and manufacture. Ellis Horwood Ltd, Chichester, pp 105–113
10. Hubbard M, Kallay M, Rowhani P (1989) Three dimensional bobsled turning dynamics. Int J Sports Biomech 5:222–237
11. Kelly A, Hubbard M (2000) Design and construction of a bobsled driver training simulator. Sports Eng 3:13–24
12. Zhang YL, Hubbard M, Huffman RK (1995) Optimum control of bobsled steering. J Optim Theory Appl 85:1–19
13. Gallier JA (2002). http://www.seas.upenn.edu/cis70005. Accessed Dec 2011
14. Kane TR, Levinson DA (1985) Dynamics: theory and applications. McGraw-Hill, New York
15. Mössner M, Hasler M, Schindelwig K, Kaps P, Nachbauer W (2011) An approximate simulation model for initial luge track design. J Biomech 44(5):892–896
16. Balakin VA, Smirnov VN, Pereverzeva OV (1988) Sliding of sled runner over ice. Friction Wear 9(2):266–273